MICROBIOLOGY

Low functional change despite high taxonomic turnover characterizes the *Ulva* microbiome across a 2000-km salinity gradient

Luna M. van der Loos[1,2]*, Sophie Steinhagen[3], Willem Stock[1], Florian Weinberger[4], Sofie D'hondt[1], Anne Willems[2], Olivier De Clerck[1]

The green seaweed *Ulva* relies on associated bacteria for morphogenesis and is an important model to study algal-bacterial interactions. *Ulva*-associated bacteria exhibit high turnover across environmental gradients, leading to the hypothesis that bacteria contribute to the acclimation potential of the host. However, the functional variation of these bacteria in relation to environmental changes remains unclear. We analyzed 91 *Ulva* samples across a 2000-kilometer Atlantic–Baltic Sea salinity gradient using metagenomic sequencing. Metabolic reconstruction of 639 metagenome-assembled genomes revealed widespread potential for carbon, nitrogen, sulfur, and vitamin metabolism. Although the R^2 value for salinity explained 70% of taxonomic variation, it accounted only for 17% of functional variation. The limited variation was attributed to typical high-salinity bacteria exhibiting enrichment in genes for thiamine, pyridoxal, and betaine biosynthesis, which likely contribute to stress mitigation and osmotic homeostasis in response to salinity variations. Our results emphasize the importance of functional profiling to understand the seaweed holobiont and its collective response to environmental change.

INTRODUCTION

Microbial communities interact with eukaryotic hosts in every ecosystem, yet our understanding of how (variation in) microbial metabolisms affect host performance is very limited. In seaweeds, host health, reproduction, and development are strongly dependent on the associated symbionts. Beyond the exchange of key nutrients, vitamins, and secondary metabolites, the microbial biofilm forms a physical and chemical barrier acting as a "second skin" that protects the host and modulates its interactions with the environment (*1*, *2*). Beneficial bacteria can shield the host against pathogens (*3*), stimulate algal growth (*4*), or mitigate the adverse effects of environmental pollution (*5*).

Species of the green seaweed *Ulva* are particularly well studied and serve as a model for algal-bacterial interactions (*6*). The relation between *Ulva* and its symbionts, collectively known as a holobiont, is so indispensable that the seaweed fails to develop its typical leaf- or tube-like morphology in the absence of particular bacteria (*7*). Morphological development is induced by chemical compounds produced by bacteria that trigger cell wall development, rhizoid formation, and cell division (*8*). Initial studies identified a combination of two complementary strains (a *Roseovarius* and a *Maribacter* strain) that were necessary for full morphogenesis in *Ulva mutabilis*. Since then, multiple strains have been identified that have the same capacity (*9*). This functional redundancy across taxa is important for the host in relation to shifts in bacterial communities.

Seaweed-associated bacterial communities are dynamic, fluctuating through time and space (*10*, *11*). Although a small core community can sometimes be identified, factors like temperature, light, salinity, and the physiology of the host itself influence community composition (*12*, *13*). Prior research has mainly focused on dynamics in the taxonomic composition of the communities rather than the functional potential that the community harbors. Taxonomic profiling using 16*S* ribosomal RNA (rRNA) amplicon sequencing has become widely accessible in recent years due to increased speed and reduced costs. In contrast, metagenomic sequencing, which provides functional insights, is more expensive. Functional profiling of bacterial communities in seaweeds like *Sargassum* (*14*, *15*), *Pyropia haitanensis* (*16*), and *Nereocystis luetkeana* (*17*) highlighted the importance of bacterial biofilms in vitamin production, polysaccharide degradation, and nutrient cycling. However, these studies were based on a relatively small number of replicates (between three and seven samples) and therefore do not capture differences across environments. To understand how the functional potential of a bacterial community responds to environmental change and to evaluate the potential consequences for the seaweed host, broader functional profiling across environmental gradients is needed (*18*).

Ulva species thrive in a range of salinities, from freshwater to highly saline conditions. The Baltic Sea, which hosts over 15 *Ulva* species across a 2000-km salinity gradient, is a particularly interesting area to study these seaweeds and their microbiome (*19*). The distribution of some *Ulva* species is confined to higher salinities, whereas other species like *U. intestinalis* and *U. linza* can be found throughout the entire range. A previous study showed that salinity strongly structures the taxonomic composition of *Ulva*-associated bacterial communities (*20*). The question remains, however, whether these taxonomic shifts are reflected by corresponding changes in functional profile of the same bacterial communities or whether functional traits are conserved across the environmental gradient.

To address these knowledge gaps and enhance our understanding of the *Ulva* holobiont model system, we investigated the taxonomic and functional composition of *Ulva*-associated bacteria across the Baltic Sea–Atlantic salinity gradient using metagenomic sequencing. The aim of this study was twofold: (i) to provide a comprehensive

[1]Phycology Research Group, Department of Biology, Ghent University, Ghent, Belgium. [2]Laboratory of Microbiology, Department Biochemistry and Microbiology, Ghent University, Ghent, Belgium. [3]Department of Marine Sciences-Tjärnö, University of Gothenburg, SE-452 96 Strömstad, Sweden. [4]GEOMAR Helmholtz Centre for Ocean Research Kiel, 24148 Kiel, Germany.
*Corresponding author. Email: luna.vanderloos@ugent.be

overview of the functional potential within the *Ulva* bacteriome based on a large number of samples ($n = 91$) and (ii) to assess whether the functional potential of the microbial community was stable across an environmental gradient. We expected that the functional repertoire of *Ulva*-associated bacteria would be rich in carbon utilization and nutrient cycling pathways as these functions are traditionally associated with seaweed microbiomes (*16*, *17*). Given that salinity has been identified as a major driving force of global bacterial diversity and community structure (*21*), we also hypothesized pronounced changes in the functional profile of the *Ulva*-associated bacterial community, particularly in functions related to osmoprotection.

RESULTS AND DISCUSSION

Ulva-associated bacteria use host-derived carbon and sulfur

We used metagenomic sequencing to comprehensively describe the functional profile of *Ulva*-associated bacteria, obtaining a large dataset of metagenome-assembled genomes (MAGs) that were annotated with the Carbohydrate-Active EnZymes (CAZy) database (*22*) and Kyoto Encyclopedia of Genes and Genomes (KEGG) (*23*, *24*). Across 91 *Ulva* microbiome samples (table S1) and 639 MAGs (table S2), we identified a total of 6425 KEGG Orthology (KO) terms and 399 KEGG modules (table S3). MAGs with an estimated completeness of >90% contained on average 59 KEGG modules (ranging from 33 to 94 modules). Apart from basic cellular metabolic pathways [e.g., fatty acid biosynthesis, RNA polymerases, DNA polymerases, ribosome, F-type adenosine triphosphatases (ATPases), cytochrome c oxidase, etc.], the *Ulva*-associated bacterial communities contained a range of functions that are clearly linked to the association with its host. This included the widespread potential of bacteria to use host-derived carbon and sulfur.

All 639 MAGs were able to use organic carbon as their primary energy source through, e.g., complex carbon degradation, glycolysis (KEGG modules M00001+M00002), and the tricarboxylic acid cycle (M00009) (Fig. 1A). Likewise, many bacteria were capable of using sulfur compounds produced by the host. Sulfur metabolism related genes in *Ulva*-associated communities were predominantly involved with assimilatory sulfate reduction (M00176), leading to the formation of sulfite and, ultimately, sulfide (Fig. 1A). In addition, 137 MAGs were able to oxidize thiosulfate (the result of the incomplete oxidation of sulfides) through sulfur-oxidizing proteins SoxAB and SoxXYZ that together form the Sox complex (M00595) (Fig. 1A). Because of the presence of sulfate esters in cell wall polysaccharides, *Ulva* species have a relatively high sulfur content (*25*, *26*) and our findings support the hypothesis that the widespread prevalence of sulfonates in marine algae contributes to the high abundance of sulfonate-degrading bacteria in marine habitats (*27*).

Other prevalent sulfur cycling enzymes in *Ulva*-associated bacteria were related to dimethylsulfoniopropionate (DMSP) metabolism, an organosulfur compound produced by *Ulva* (*28*, *29*). DMSP has a wide range of ecophysiological functions, and in the model species *U. mutabilis*, it is known to mediate the interaction with the symbiont *Roseovarius* sp. MS2. This symbiont releases morphogenetic compounds that stimulate algal morphogenesis and growth (*30*). Although the bacterial strain is attracted by the release of DMSP and rapidly takes up the compound, its growth is not affected by DMSP. Instead, DMSP is converted into dimethyl sulfide (DMS) and methanethiol (MeSH). In our dataset, the capacity to convert DMSP to DMS was almost exclusively restricted to a few genera within the *Rhizobiaceae* (the undescribed genus JAALLB01) and *Rhodobacteraceae* (predominantly *Jannaschia*, *Roseovarius*, and *Sulfitobacter*). This observation aligns with previous findings that another well-known

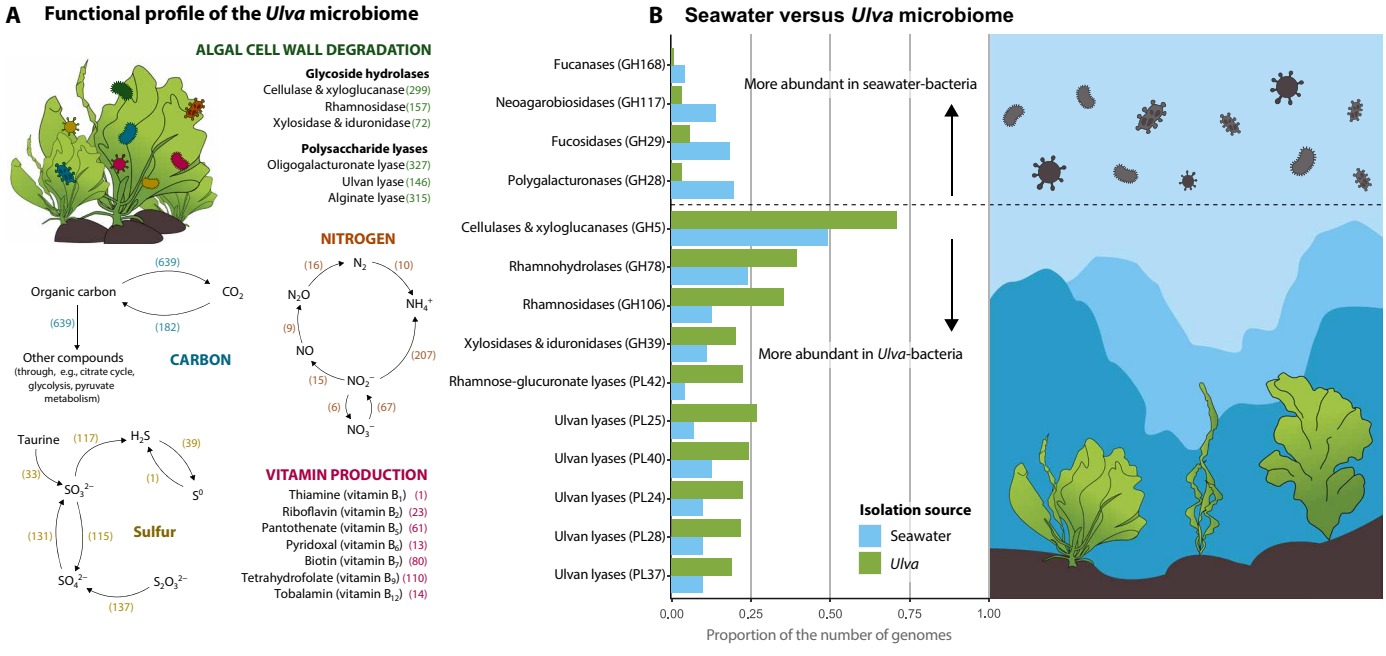

Fig. 1. Functional profile of the *Ulva* microbiome. (**A**) Overview of the metabolic potential of the *Ulva* microbiome, highlighting vitamin production (purple), algal cell wall degradation (green), and the metabolism of carbon (blue), nitrogen (orange), and sulfur (yellow). The number of identified MAGs that are capable performing the reactions is displayed in parentheses. (**B**) Proportion of the number of seawater-isolated (blue) or *Ulva*-isolated (green) bacterial genomes that contained a specific CAZy family (polysaccharide lyases, PL; glycoside hydrolases, GH).

morphogenesis-inducing symbiont of *Ulva*, *Maribacter* sp. MS6 (belonging to the *Flavobacteriaceae*), is not attracted by DMSP (*30*).

In addition to examining carbon and sulfur metabolic functions via KEGG modules, we screened *Ulva*-associated bacterial MAGs for carbohydrate-active enzymes using the CAZy database. CAZy categorizes enzymes involved in degrading, modifying, or creating glycosidic bonds into families, including glycoside hydrolases (GHs) and polysaccharide lyases (PLs). We identified 121 GH families and 26 PL families within *Ulva*-associated MAGs. Our results demonstrated that 97% of these bacteria are capable of breaking down complex polysaccharides in the *Ulva* cell wall, composed mainly of cellulose, glucuronan, ulvan, and xyloglucan, which together make up 45% of the dry-weight biomass (*31*). Ulvan, a key component, is composed of sulfated rhamnose, xylose, and uronic acids (D-glucuronate and iduronic acid) (*31*). The initial steps in the breakdown of ulvan can be catalyzed by ulvan lyases (sulfatases) (*32*), but additional GHs are needed to obtain monomeric sugars (*33*). Ulvan lyases (CAZy families PL24, PL25, and PL37 among others) were found in 146 MAGs (Fig. 1A), many of which were typical *Ulva*-associated bacteria, such as *Lewinella*, *Nonlabens*, *Algibacter*, *Glaciecola*, and *Polaribacter* (*9*). Prevalent GH families included GH3 (553 MAGs), GH16 (305 MAGs), and GH5 (299 MAGs). Family GH3 includes, among others, xyloglucan-specific exo-β-1,4-glucosidase (EC 3.2.1.-), xylan β-1,4-xylosidase (EC 3.2.1.37), several glucanases, and several other glucosidases. Enzymes of family GH16 are active on β-1,4 or β-1,3 glycosidic bonds in various glucans and galactans and includes xyloglucan:xyloglucosyl transferase (EC 2.4.1.207). Members of the GH5 family are mainly active on cellulose, but this family also includes high-specificity xyloglucanases.

Nitrogen metabolism and amino acid biosynthesis

Unlike animals, seaweeds can synthesize essential amino acids and relatively little is known about the uptake of dissolved organic nitrogen compounds by seaweeds (*34*). It is likely, however, that seaweeds and bacteria do exchange amino acids, especially when dissolved inorganic nitrogen availability is low (*35*). The biosynthesis of multiple amino acids was part of the core modules of the *Ulva*-associated bacteria (with 0.65 to 1.42% relative abundance in at least 99% of samples). This included the biosynthesis of proline (KEGG module M00015), threonine (M00018), lysine (M00016, M00526, and M00527), valine/isoleucine (M00019), serine (M00020), cysteine (M00021), tryptophan (M00023), histidine (M00026), ornithine (M00028), leucine (M00432), and arginine (M00844). Of these core modules, cysteine biosynthesis was detected in the fewest number of MAGs (222 MAGs), whereas histidine biosynthesis was found in the highest number of MAGs (443 MAGs). Likewise, genes necessary for glycine biosynthesis (from threonine or serine), alanine biosynthesis (from pyruvate), and glutamine biosynthesis (from glutamate), as well as the conversion between aspartate and asparagine, were prevalent in most MAGs.

Nitrogen metabolism potential largely centered on the conversion from nitrate and nitrite to ammonia (Fig. 1A). A large number of 174 MAGs contained *nrfAH* or *nirBD* genes essential for this process. Thirty MAGs exhibited the genes for full dissimilatory nitrate reduction to ammonia, using nitrate respiration for energy production (M00530). Only seven MAGs, all Cyanobacteria, demonstrated complete assimilatory nitrate reduction capability, involving the reduction of nitrate to ammonia for biosynthesis purposes (M00531). Nevertheless, the first step in this process (nitrate to nitrite reduction mediated by *narB*) was identified in 53 MAGs, and the subsequent step (nitrite to ammonia reduction facilitated by *nirA*) was detected in 45 MAGs. *narB* was predominantly observed in *Flavobacteriaceae* and *Saprospiraceae*, whereas *nirA* was prevalent in *Akkermansiaceae* and *Pirellulaceae*. Two MAGs harbored all the genes necessary for denitrification, involving the reduction of nitrate and nitrite to nitrogen (M00529), whereas none of the MAGs carried genes associated with nitrification (the oxidation of ammonia to nitrate; M00528). Last, 10 MAGs from various families showed the capacity to fix nitrogen (M00175).

Previous studies demonstrated that observed amino acid uptake rates in *Ulva* were highest for glycine and alanine and that, although *Ulva* prefers inorganic nitrogen, the organic compounds may also play a substantial role (*36*, *37*). A transcriptomic study in *Laurencia dendroidea* showed that the associated bacteria had a higher relative contribution to amino acid metabolism than the host itself, indicating a symbiotic relation (*38*). Similarly, in *P. haitanensis*, cocultivation with a *Bacillus* sp. did not only result in an increased growth rate but also in the down-regulation of genes related to the biosynthesis of several amino acids and other metabolites (*39*). As free amino acids are known to increase primary production of algae (*40*, *41*), it is hypothesized that the release of amino acids by bacteria serves as one mechanism through which they may facilitate algal growth.

Large potential for vitamin B production by bacteria

Previous metagenomic studies in the red alga *P. haitanensis* (*16*) and brown alga *N. luetkeana* (*17*) have highlighted the potential of the bacterial symbionts to produce vitamin B_{12} (cobalamin). Our data showed that the capacity of seaweed-associated bacteria to biosynthesize vitamins is widespread within the *Ulva* microbiome and extends beyond vitamin B_{12} (Fig. 1A). Vitamins are essential to a well-functioning central metabolism in both microbes and their hosts (*42*, *43*). Algae require a combination of different vitamins for growth but are likely unable to synthesize some of these organic compounds (*44*–*46*). A study by Croft *et al.* (*47*), for example, showed that more than half of the algae studied by them required an exogenous supply of vitamin B_{12} (cobalamin), 22% required vitamin B_1 (thiamine), and 5% required vitamin B_7 (biotin). In *Ulva* species, the addition of vitamin B_{12} and, particularly, vitamin B_6 (pyridoxal) to a culture medium is necessary for growth and promotes nitrogen metabolism (*48*, *49*). This vitamin auxotrophy suggests that the host is dependent on the production by its microbial symbionts. Within our dataset, the capacity of bacteria to produce tetrahydrofolate (a derivative of vitamin B_9; KEGG module M00126) was most widespread and was identified in 110 MAGs from varying families, including the *Alteromonadaceae*, *Flavobacteriaceae*, *Granulosicoccaceae*, *Saprospiraceae*, and *Spirosomaceae* (Fig. 1A). This was the only vitamin that was part of the core functions of the *Ulva* microbiome, being consistently present in all samples with a minimum relative abundance of 0.1%. KEGG modules related to the production of vitamin B_1 (thiamine; M00127), vitamin B_2 (riboflavin; M00125), vitamin B_5 (pantothenate; M00119), vitamin B_6 (pyridoxal; M00124), vitamin B_7 (biotin; M00123), and vitamin B_{12} (cobalamin; M00122) were identified as well (Fig. 1A) although not as core functions. This could be attributed to either the absence of MAGs with the capacity to produce these vitamins in all samples or to their lower abundance across all samples.

The *Ulva* microbiome is defined by its ability to degrade the host

Our metagenomic dataset provided a thorough overview of the functional profile of the *Ulva*-associated microbiome. Next, we aimed to

determine the functions contributing to a "typical" *Ulva* microbiome, by contrasting taxa isolated from *Ulva* with those isolated from seawater. In total, we selected 152 MAGs from our metagenomic dataset, representing 33 different genera (table S4). We then searched for publicly available genomes of bacteria from the same genera but isolated from seawater (71 genomes) (table S4). Subsequently, we conducted a comparative analysis based on odds ratios to identify potential enrichments of specific KO terms or CAZys in bacteria from the same genus collected from *Ulva* versus seawater.

Our results suggest that a defining aspect of an *Ulva* microbiome is its ability to use and break down the host organism, shown by the significant enrichment of CAZys (including ulvan lyases, α-L-rhamnosidases, and rhamnogalacturonan α-L-rhamnohydrolase) that specifically target and break down *Ulva*'s polysaccharides and cell wall components (e.g., ulvan, iduronic acid, cellulose, and xyloglucan) (Fig. 1B), as well as ABC (adenosine triphosphate–binding cassette) transporters that facilitate the extracellular uptake of small monosaccharides like fructose (*frcBCA*; KEGG KO K10552, K10553, and K10554), α-glucoside (*aglEFGK*; K10232, K10233, and K10234), and rhamnose (*rhaSPQT*; K10559 and K10560) resulting from the degradation of the cell wall polysaccharides. It is clear that *Ulva*-associated bacteria do not only live on the algal tissue, but they also live off it as well.

High taxonomic turnover and functional redundancy across salinity gradient

Subsequently, we examined the shifts in both the taxonomic and functional composition of *Ulva*-associated bacteria across a salinity gradient spanning from the horohalinicum [5 to 8 practical salinity unit (PSU)], through the mesohaline (8 to 18 PSU) and the polyhaline (18 to 30 PSU), to the euhaline (30 to 35 PSU) (Fig. 2A). The Atlantic–Baltic Sea salinity gradient explained more of the observed variation in the taxonomic composition of *Ulva*-associated bacterial communities ($P = 0.0001$, $R^2 = 0.70$; vegan envfit) than that of the observed variation in the functional composition of the same communities ($P = 0.0006$, $R^2 = 0.17$; vegan envfit) (Fig. 2, B to G). Pairwise comparisons, for example, showed that the taxonomic composition of *Ulva*-associated bacteria differed between all salinity regions (horohalinicum versus mesohaline versus polyhaline versus euhaline, $P < 0.01$ for all comparisons; pairwise Adonis test). On the other hand, the functional gene profile of bacterial communities in the mesohaline, polyhaline, and euhaline were not significantly different from each other ($P > 0.05$ for

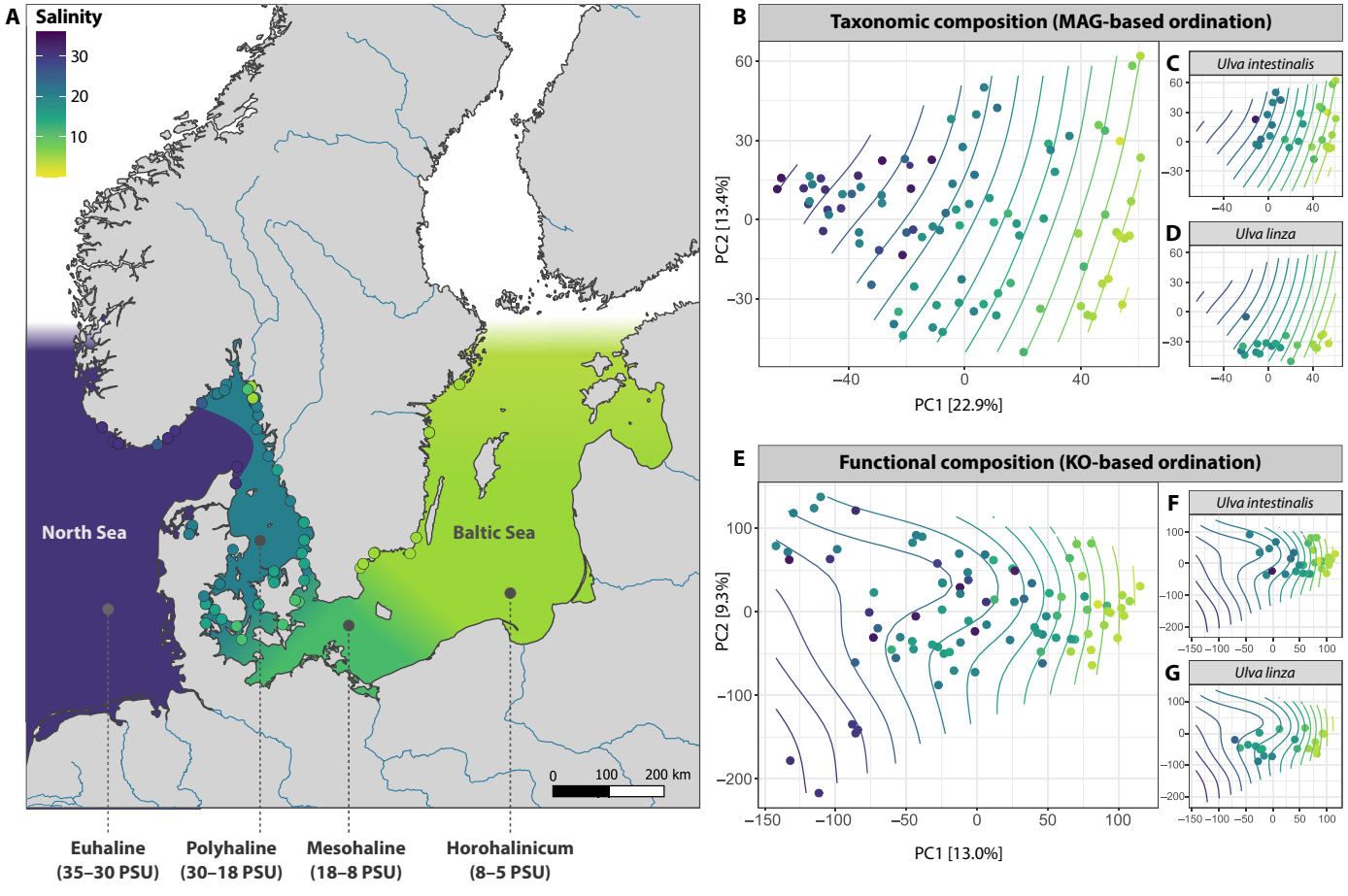

Fig. 2. Taxonomic and functional patterns across salinity. (**A**) Geographic distribution of sampling sites ($n = 63$) along the Atlantic–Baltic Sea gradient where a total of 91 *Ulva sensu lato* samples were collected. The four major salinity regions (horohalinicum, mesohaline, polyhaline, and euhaline) have been indicated on the map, and rivers are projected in blue. PCA plots show the taxonomic (**B** to **D**) and functional (**E** to **G**) composition of *Ulva*-associated bacterial communities across salinity. The ordination in the taxonomic composition is MAG-based, and the functional composition is KO-based. The contour lines (smooth surface lines) were fitted to the ordination plots based on the correlation with salinity. Color represents salinity in all plots.

all comparisons, pairwise Adonis test) as only the horohalinicum differed from the two higher salinity regions (horohalinicum versus polyhaline, $P = 0.04$; horohalinicum versus euhaline, $P = 0.04$, pairwise Adonis test).

Nutrient concentrations, temperature, and oxygen concentrations had little to no effect on taxonomic turnover (NO_x, $P = 0.03$, $R^2 = 0.07$; PO_4, $P = 0.08$, $R^2 = 0.05$; temperature, $P = 0.01$, $R^2 = 0.10$; and oxygen, $P = 0.18$, $R^2 = 0.04$; vegan envfit) and did not affect functional composition (NO_x, $P = 0.90$, $R^2 = 0.002$; PO_4, $P = 0.22$, $R^2 = 0.03$; temperature, $P = 0.16$, $R^2 = 0.04$; and oxygen, $P = 0.83$, $R^2 = 0.004$; vegan envfit).

Indicative of a high taxonomic turnover, 294 MAGs changed in relative abundance across the salinity gradient ($P < 0.01$, LinDA linear regression) (Fig. 3A and table S2), of which 126 MAGs decreased with salinity and 168 MAGs increased with salinity. Several MAGs belonging to *Dokdonia* (MAG082 and MAG518), *Leucothrix* (MAG022 and MAG360), and *Litorimonas* (MAG193 and MAG149), for example, increased with salinity, whereas *Alteraurantiacibacter* (MAG014, MAG020, and MAG578), *Rubripirellula* (MAG422), and *Blastomonas* (MAG197) decreased with salinity (Fig. 3B).

A previous study using a 16*S* rRNA gene dataset, collected across the same Atlantic–Baltic Sea environmental gradient (*20*), showed that *Ulva*-associated bacterial communities were strongly structured not only by salinity but also secondarily by host species. Our MAG-based metagenomic dataset likewise demonstrated that different *Ulva* species hosted distinct microbial communities ($P < 0.0001$, $R^2 = 0.58$; vegan envfit) (Fig. 2, C and D), which also exhibited varying functional profiles ($P < 0.0001$, $R^2 = 0.41$; vegan envfit) (Fig. 2, F and G). As several *Ulva* species exclusively occurred in the polyhaline and euhaline regions of the salinity gradient, the variation explained by salinity and host species partly overlaps. Two species, *U. intestinalis* and *U. linza*, co-occurred across the entire salinity gradient and provide a good case study to disentangle the effects of host and salinity. If only salinity is taken into account, 134 MAGs were found to significantly change in abundance with salinity ($P < 0.01$, LinDA linear regression, model: ~ salinity + NO_x + PO_4 + temperature + O_2). However, if host differences are also taken into account, an additional 46 MAGs were found with fluctuating abundances, caused by the interaction between the host and salinity variables (Fig. 4A). MAG372 (*Akkermansiaceae*) and MAG451 (Bacteroidia NS11-12g), for example, decreased strongly across the salinity gradient, but only in *U. linza* (Fig. 4C). Conversely, MAG365 (*Lewinella*) only decreased with salinity in *U. intestinalis* communities (Fig. 4C). MAG402 (*Saprospiraceae*) increased across salinity in both host species but was generally more abundant in *U. linza*, whereas MAG411 (*Mauriculaceae*) was more abundant in *U. intestinalis* (Fig. 4C). We also identified 127 MAGs that did not change across salinity but were enriched in *U. intestinalis* communities (Fig. 4B) and 55 typical *U. linza* MAGs (Fig. 4D).

The taxonomic turnover was larger than the observed shift in functional potential, implying that multiple taxa across the salinity gradient were able to perform similar functions. Figure 5 gives a complete overview of the presence or absence of KEGG modules in the MAGs of 26 taxa that are characteristic to a specific salinity region (horohalinicum: 5 to 8 PSU, mesohaline: 8 to 18 PSU, polyhaline: 18 to 30 PSU, or euhaline: 30 to 35 PSU). Pantothenate (vitamin B_5), for example, can be produced at low to medium salinity (5 to 18 PSU) by an unknown *Saprospiraceae* (MAG591), but at medium to high salinity (18 to 35 PSU), this function in the community was taken over by *Robiginitomaculum* and another unknown *Saprospiraceae* (MAG149) (Fig. 5). Similarly, proline biosynthesis at low salinity can be conducted by *Alteraurantiacibacter* and *Rubripirellula* (5 to 8 PSU) and at medium salinity by *Litorimonas* A (8 to 18 PSU) and was gradually taken over by *Neomegalonema* (18 to 30 PSU) and *Leucothrix* and *Litorimonas* at high salinity (30 to 35 PSU). In addition, most MAGs shared a set of core genes that are necessary for essential functions, including nucleotide metabolism, fatty acid biosynthesis, energy metabolism (F-type ATPases, succinate dehydrogenases, etc.), and genes encoding structural modules (e.g., ribosomes, RNA polymerase, and DNA polymerase) (Fig. 5). The number of core genes varies depending on whether these are calculated across MAGs (i.e., taxa) or across microbial communities (i.e., samples). Only 3.4% of all KOs were shared among 95% of the MAGs in our dataset (considering only MAGs with genome completeness of >90%). This percentage increased to 7.7% for genes shared by at least 80% of MAGs and further increased to 13.6% for genes shared by at least 50% of MAGs. In contrast, when compared across microbial communities, these numbers are much higher: 35.4% of KOs were shared by 95% of microbial communities in our dataset, 42.7% were shared by 80% of the microbial communities, and 52.1% of genes were shared by 50% of the microbial communities. This again emphasizes the presence of functional redundancy in microbial communities associated with *Ulva* across the studied salinity gradient.

Osmoregulation drives functional variation

Despite lower functional turnover, we also identified 23 KEGG modules that differed in abundance across the salinity environment ($P < 0.05$, LinDA linear regression) (Fig. 6). These modules are likely involved in the osmoregulation of bacterial cells but may also affect the osmoregulation and acclimation potential of the host. One of the best-known strategies in bacteria and eukaryotes alike is the accumulation of low–molecular weight compounds, such as sugars and amino acids, that act as osmoprotectants to maintain osmotic homeostasis and turgor pressure. Other strategies included the stabilization of cell membranes and mitigating oxidative stress.

Salinity-induced osmotic changes trigger the overproduction of reactive oxygen species (ROS), causing oxidative stress (*50*) and damaging membrane lipids, proteins, nucleic acids, and chloroplasts (*51*). Bacteria abundant in high-salinity areas more often had genes needed to produce cofactor F_{420} (KEGG module M00378, $P = 0.0004$; LinDA linear regression), thiamine (vitamin B_1; KEGG module M00127, $P < 0.0001$; LinDA), and pyridoxal-5P (the active form of B_6; M00124, $P = 0.001$; LinDA). Several antioxidant mechanisms are F_{420} dependent (*52*), and cofactor F_{420} is known to help bacteria combat oxidative stress (*53*). Both vitamins B_1 and B_6 are known to alleviate salinity stress in plants like *Arabidopsis thaliana* (*54*) and milk thistle (*55*), by enhancing antioxidant enzyme activity and proline content. Similarly, vitamin B_1 gene expression is up-regulated in phytoplankton during salt stress, suggesting its role as a stress signaling molecule (*56*, *57*). Pyridoxal-5P not only protects against oxidative stress but also increases photosynthetic pigment in wheat (*58*), and it facilitates growth through the reduction of ethylene accumulation that usually occurs under salinity stress in rice (*59*). As algae are likely not always able to produce their own vitamins (*44*), it is possible that thiamine and pyrodixal-5P produced by bacteria also aid the *Ulva* cells against oxidative radicals that are more prevalent under high-salinity levels.

Bacteria abundant in high-salinity areas more often contained genes for betaine production (M00555, $P = 0.03$; LinDA linear regression), an

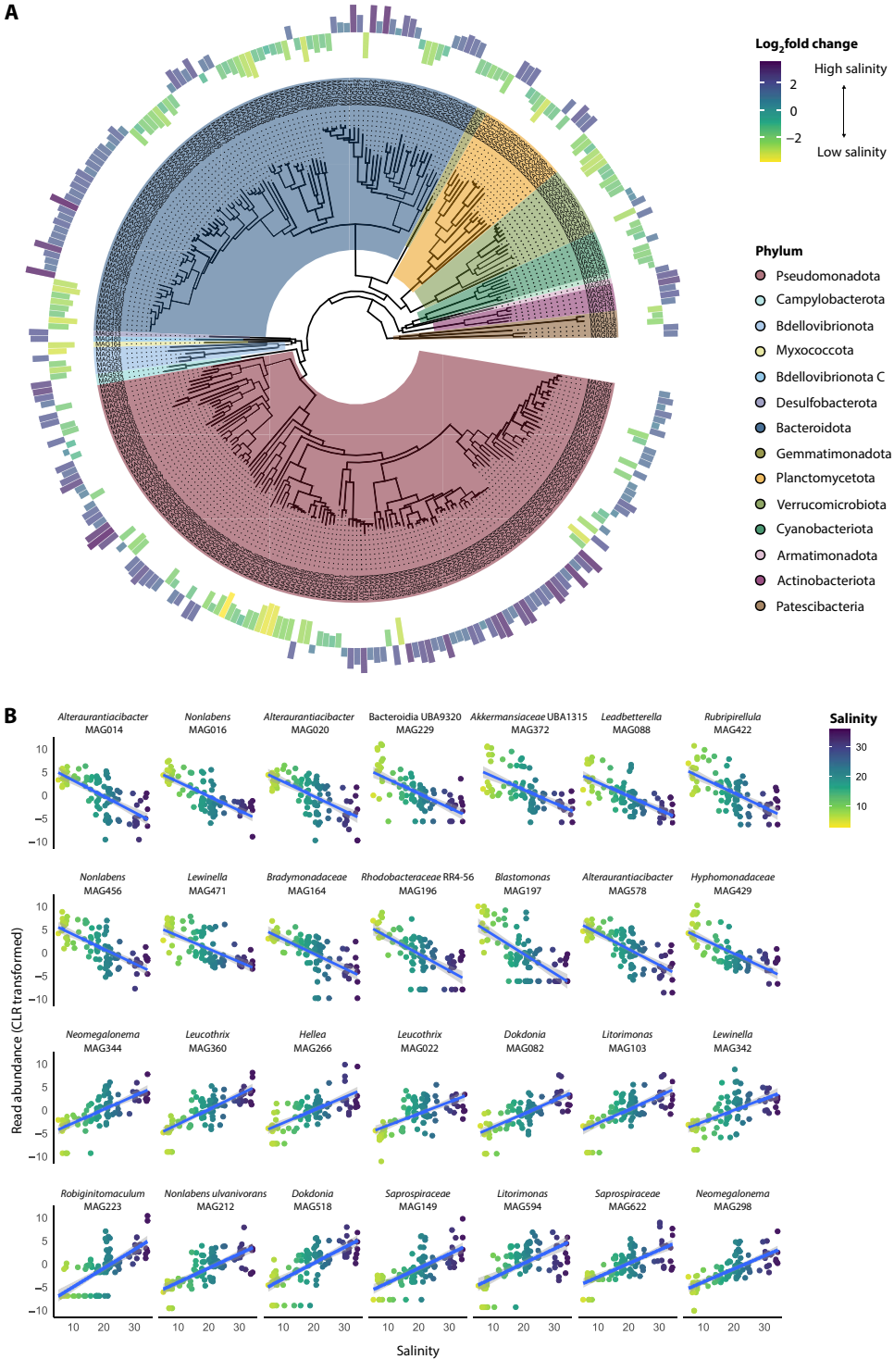

Fig. 3. Abundance of MAGs across salinity. (**A**) Phylogenetic tree of the 294 MAGs that significantly differed ($P < 0.01$) in relative abundance across the salinity gradient. The outer ring represents the $\log_2$fold change (LinDA linear regression model with $n = 91$ samples), with the MAGs in yellow-green that are enriched in low salinity and the MAGs that are enriched in high salinity in purple-blue. The colors in the phylogenetic tree represent the bacterial phyla (the legend is ordered in clockwise order of appearance). (**B**) Read abundance of the 28 most differentially abundant MAGs across salinity. The *x* axis displays salinity (PSU), and the *y* axis CLR-transformed read abundance. Colors represent salinity. Curves were fitted with a generalized linear model (GLM) using the R package ggplot2. Shaded areas represent the 0.95 confidence interval.

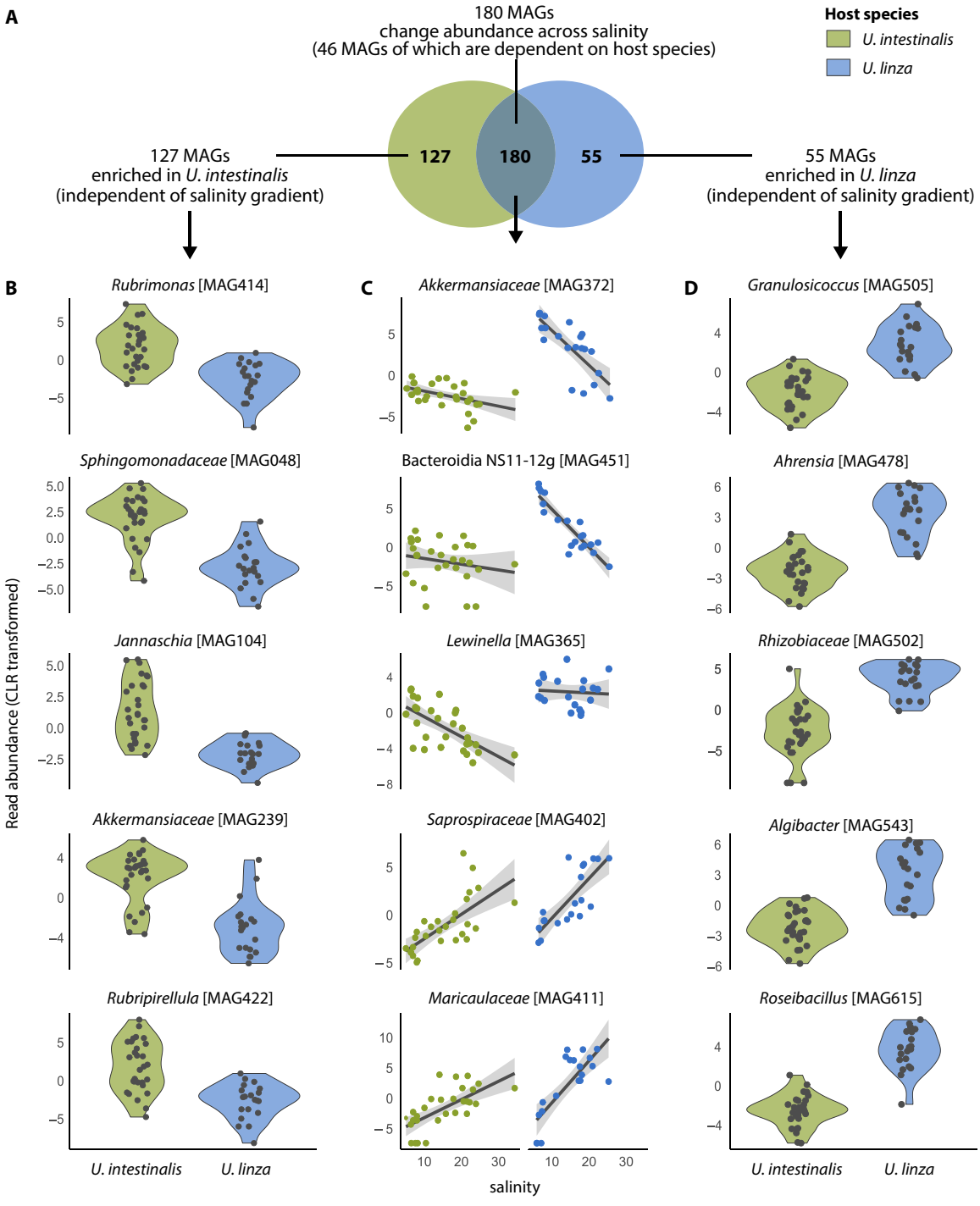

Fig. 4. Interactive effects between salinity and host species. (**A**) Venn diagram displaying the number of MAGs that (i) were enriched in *U. intestinalis* communities independent of salinity, (ii) were enriched in *U. linza* communities independent of salinity, and (iii) displayed changes in abundance across salinity in at least one of the host species (LinDA linear regression models with $n = 49$ samples and significant values determined as $P < 0.01$). (**B** to **D**) Five examples from MAGs of each of the three Venn categories. Violin plots in (B) and (D) depict CLR-transformed (centered log-ratio) read abundance for both host species. Scatterplots in (C) depict CLR-transformed read abundance across salinity (PSU). Curves were fitted with a GLM using the R package ggplot2. Shaded areas represent the 0.95 confidence interval. Colors indicate host species: *U. intestinalis* (green) and *U. linza* (blue).

Fig. 5. Taxonomic turnover and functional redundancy. Heatmap depicting the presence (dark green) or absence (light blue) of KEGG modules in 26 MAGs that are characteristic to a specific salinity region (horohalinicum: 5 to 8 PSU; mesohaline: 8 to 18 PSU; polyhaline: 18 to 30 PSU; or euhaline: 30 to 35 PSU).

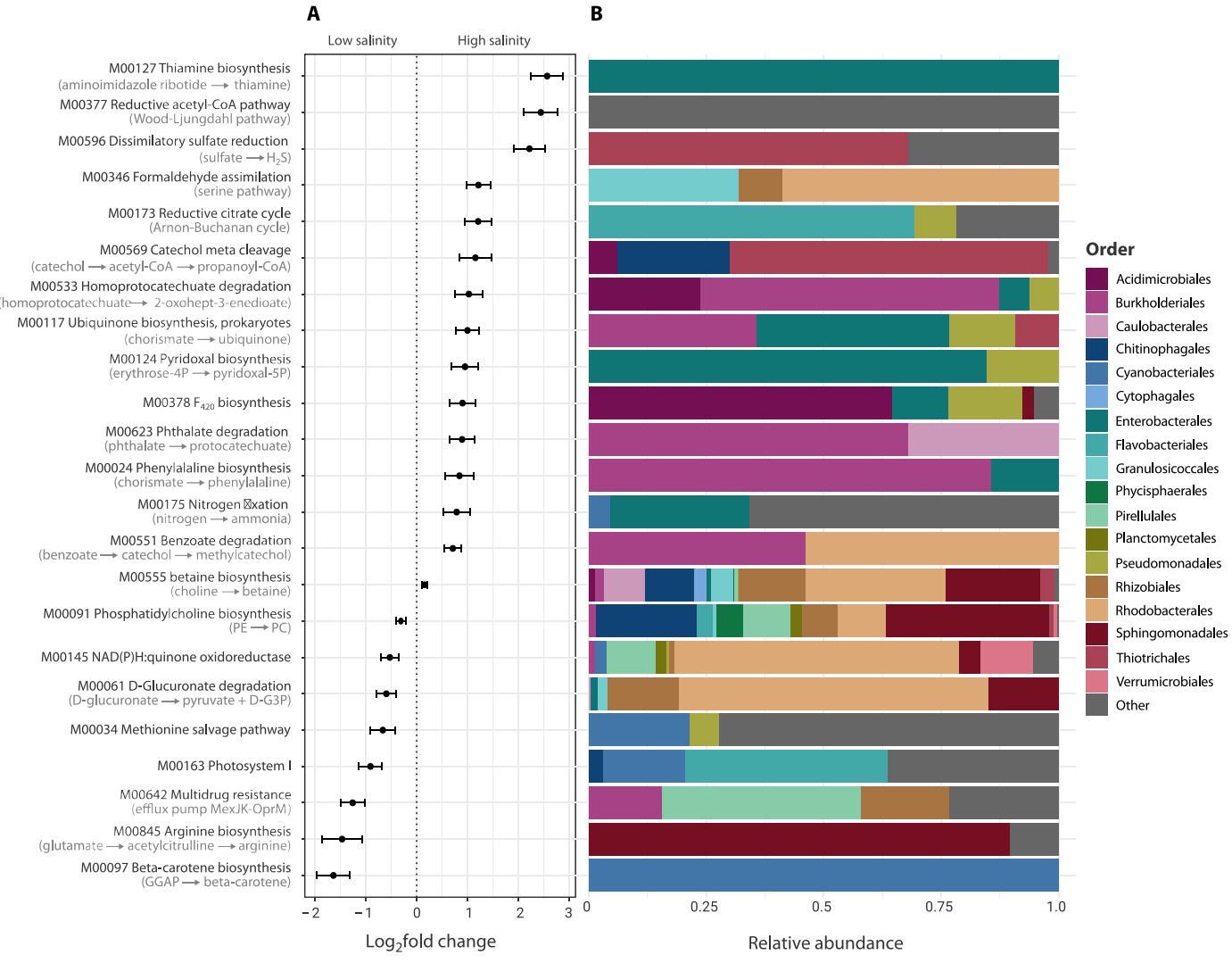

Fig. 6. Functional changes in the *Ulva*-associated bacterial communities across salinity. (**A**) Log_2fold change values (± SE) of the KEGG modules that significantly ($P < 0.05$) differed in abundance with salinity. (**B**) Taxonomic composition (order level) of the MAGs that harbored the identified KEGG modules. The relative abundance is based on read counts of the orders across the entire dataset.

osmolyte that acts as one of the preferred compatible solutes in most prokaryotes (*60*, *61*). It is known to accumulate in bacterial cells with increasing salinity (*62*), and betaine transporters are enriched in bacterial communities originating from marine habitats compared to freshwater environments (*63*). Although betaine primarily acts as osmoprotectant in higher plants rather than algae (*64*), a transcriptomic study in *Ulva compressa* showed that three choline dehydrogenase genes (involved in the conversion from choline to betaine) were up-regulated during a recovery period after hyposaline stress (*65*). We also observed an enrichment of bacterial genes for producing phenylalanine, an essential amino acid that accumulates in plants and algae under high salinity (*66*, *67*) and increases salinity tolerance in maize (*68*). Genes associated with biosynthesis of other well-known osmolytes and osmoprotectants, such as ectoine and trehalose, were comparatively less prevalent in our dataset.

Another well-known strategy of bacteria to cope with cell turgor pressure is to alter the membrane composition through changes in fatty acids or phospholipids (*69*). The cell membrane separates the cell's interior from the external environment and is therefore the first structure to encounter the effects of fluctuating salinity and osmotic stress. Membrane disruption affects many processes such as transport of compounds, enzyme activities, and signal transduction. It is therefore important to maintain the correct fluidity of the lipid bilayer (*70*). We found that many typical high-salinity MAGs were associated with the ability to synthesize ubiquinone (M00117, $P = 0.02$; LinDA linear regression), which agrees with the findings by Dupont *et al.* (*63*) on pelagic bacterial communities. Ubiquinone (also called coenzyme Q) is a membrane-stabilizing isoprenoid, and the accumulation of this compound increases salt tolerance in bacteria, especially in the thin-walled Gram-negative bacteria (*71*, *72*). Ubiquinone alters the physicochemical properties of the membrane by increasing the lipid packing and density. This results in reduced membrane permeability (i.e., a slower release of small solutes) and increases the strength of the membrane (i.e., resistance to cell rupture) (*73*). Conversely, we found

that phosphatidylcholine (PC) biosynthesis was enriched under low-salinity conditions (M00091, $P = 0.002$; LinDA). PC is a membrane-forming phospholipid that is synthesized from phosphatidylethanolamine (PE), and studies found that PE levels increased in salt-adapted cells (*74*). Although PE is the more common phospholipid in bacteria, Gram-negative bacteria with high proportions of unsaturated fatty acids often contain additional PC to maintain stable bilayers (*75*). In our dataset, the ability to convert PE to PC was mainly found in low salinity–enriched Sphingomonadales (e.g., *Alteraurantiacibacter* and *Erythrobacter*) and Rhodobacterales (e.g., *Jannaschia* and *Pseudorhodobacter*). Membranes lacking PC are more fluid, have a higher permeability for small molecules, and are more sensitive to osmotic changes (*76*). Both quinone and PC stabilize the membrane, which is crucial to withstand changes in turgor pressure and maintain osmotic balance.

Bacteria-mediated acclimation

Our characterization of the metabolic functions of a typical *Ulva*-microbiome highlights the substantial metabolic potential inherent to bacterial-algal symbiosis. The holobiont concept, which regards the seaweed host and its associated microbes as an integrated functional unit, is essential for understanding seaweed physiological responses to environmental change. This work demonstrated that both the taxonomic and functional composition of *Ulva*-associated bacterial communities change across a 2000-km salinity gradient. Although several *Ulva* species can colonize the entire gradient, their associated bacterial taxa exhibit high turnover across salinity levels, suggesting a narrower salinity niche and limited acclimation potential compared to the host. The high turnover of microbial taxa is accompanied by functional redundancy, where guilds of taxa along the entire environmental gradient can perform crucial functions. These functions, including amino acid and vitamin B production, are potentially important to the seaweed host. Alongside functional redundancy, we identified distinct functional modules exhibiting enrichment in either low- or high-salinity areas. These modules are likely involved in mitigating oxidative stress, maintaining cellular osmotic homeostasis, and stabilizing cell membranes. *Ulva* depends on its microbiome for morphological development and growth—likewise, the aforementioned bacterial acclimation mechanisms may play a role in host metabolism and acclimation. However, it is important to keep in mind that the metagenomic data in this study only provide insights into the functional potential of the bacterial communities, indicating the presence of genes but not whether they are being actively expressed. Additional transcriptomic data are necessary to confirm active gene regulation in response to salinity fluctuations. In light of bacteria-mediated acclimation, future laboratory experiments—involving the inoculation of seaweed cultures with targeted microbial communities—will be necessary to investigate whether bacteria can facilitate the acclimation of *Ulva* species to changes in salinity.

MATERIALS AND METHODS

Sample collection

Samples of *Ulva sensu lato* individuals ($n = 91$ biological replicates) were collected during June to August 2020 in the Baltic Sea area (table S1). Of each individual, a tissue sample was collected to molecularly identify the host species and a swab sample for microbiome analyses was generated by rubbing for 30 s on the tissue. All samples were stored in a portable freezer (−20°C) until transferred to −80°C in the laboratory.

In total, 63 sampling sites were visited along a salinity gradient in the Baltic Sea and adjacent areas such as the Kattegat, Skagerrak, and the eastern North Sea (Fig. 2A). The salinity ranged from 5.1 to 34.3 PSU and is presented in the figures in this study either on a continuous scale (0 to 35 PSU) or in salinity zones defined according to the Venice classification system (5 to 8, horohalinicum; 8 to 18, mesohaline; 18 to 30, polyhaline; and 30 to 35, euhaline) (*77*). In addition, water temperature (°C), oxygen levels (mg liter^{-1}), and nutrient concentrations (NO_3^-, NO_2^-, silicate, and PO_4^{3-} in μM) were measured at each site (table S1).

Molecular identification, based on the *tuf*A marker, confirmed the samples in our dataset represented seven different species: *Blidingia minima* (Nägeli ex Kützing) Kylin ($n = 8$), *U. compressa* Linnaeus ($n = 10$), *U. fenestrata* Postels & Ruprecht ($n = 8$), *U. intestinalis* Linnaeus ($n = 29$), *U. lacinulata* (Kützing) Wittrock ($n = 10$), *U. linza* Linnaeus ($n = 20$), and *U. torta* (Mertens) Trevisan ($n = 6$) [see van der Loos *et al.* (*20*) and Steinhagen *et al.* (*19*) for detailed molecular methods and additional results concerning *Ulva* diversity in the Baltic region]. Throughout this study, "*Ulva*" refers to *Ulva sensu lato* (including *Blidingia*).

DNA extraction and metagenomic sequencing

Total microbial DNA of the swab samples was extracted with the Qiagen DNeasy Mini Kit following the manufacturer's protocol, with the addition of a bead beating step before lysis using zirconium oxide beads (RETCH Mixer mill MM400; 5 min at 30 Hz). Quantity and quality of the DNA extracts were verified with Qubit (Life Technologies, Grand Island, USA) and NanoDrop (Thermo Fisher Scientific, Wilmington, USA). DNA extracts were sent to Novogene (Cambridge, UK) for library preparation and metagenomic sequencing on an Illumina NovaSeq 6000 (150–base pair paired-end). A negative DNA extraction control and a positive control (American Type Culture Collection microbial standard MSA-1002) were included. A total of 4,297,091,260 reads were generated (35,622,356 to 78,544,930 reads per sample). The sequences are archived at the SRA (BioProject PRJNA1040445).

Bioinformatics and statistical analyses

The metagenomic sequencing data were processed with the ATLAS Snakemake workflow (*78*), integrating quality control, assembly, genomic binning, and annotation. In short, quality control, including removal of polymerase chain reaction duplicates and adapters, trimming, and filtering, was performed using the BBTools suite (*79*). Host sequences were removed based on an available *Ulva* reference genome (BioProject PRJEB25750) (*80*). MEGAHIT v1.0 was used for de novo metagenome assembly (*81*). MAGs were predicted with binning tools MetaBAT 2 (*82*) and MaxBin 2.0 (*83*), aggregated with DAS Tool (*84*), and quality assessed with CheckM (*85*). MAGs were dereplicated across samples with dRep (*86*) and taxonomically classified with GTDB-Tk (*87*). Last, genes were predicted with Prodigal (*88*), redundant genes were clustered with linclust (*89*), and annotated with eggNOG-mapper (*90*). This resulted in a classification of the genes following the CAZy database (*22*) and KEGG (*23*, *24*) databases.

The effects of salinity, NO_x, PO_4, temperature, oxygen levels, and host species on bacterial community composition at both MAG (taxonomic) and KO (functional) levels were assessed using the envfit function from the vegan package with 9999 permutations (*91*).

Multivariate comparisons were subsequently conducted with pairwise Adonis tests among different salinity zones (*92*). Taxonomic and functional differences across salinity were visualized with principal components analysis (PCA), fitting smooth surface lines to the ordination using ordisurf (vegan package) based on the salinity correlation (*91*). LinDA linear regression identified which MAGs and which KEGG modules (a set of genes with a specific reaction within a metabolic pathway) significantly changed across salinity and nutrient concentrations (*93*). To gain a better understanding of the interactive effects of host species and salinity on microbial communities, two separate LinDA linear regressions were conducted on a subset of *U. linza* and *U. intestinalis* samples ($n = 49$). The first model included only the environmental parameters (model: ~ salinity + NO_x + PO_4 + temperature + O_2), whereas the second model also included host species (model 2: ~ salinity + host + NO_x + PO_4 + temperature + O_2). All analyses on taxonomic and functional patterns included the full set of MAGs, KOs, or KEGG modules using read abundance data. Given the compositional nature of the data, read abundance values were transformed with centric log-ratios (CLRs) prior to analyses (*94*). *P* values were Bonferroni corrected.

To gain a deeper understanding of what defines the metabolic potential of *Ulva* microbiomes, we compared the genomes of bacterial taxa isolated from *Ulva* to those isolated from seawater. In total, we selected 152 MAGs from our metagenomic dataset, representing 33 different genera. We then searched for publicly available genomes of bacteria from the same genera that were isolated from seawater (resulting in a set of 71 genomes) (table S4). These originated from a variety of geographical locations and habitats (e.g., surface water, deep sea, hydrothermal systems, and oceanic gyres). Subsequently, we conducted a comparative analysis using odds ratios to identify potential enrichments of specific KO terms or CAZy families within bacteria of the same genus collected from *Ulva* versus seawater. For each KO term and CAZy family, the odds ratio was calculated as the number of discordant genome pairs in favor of the *Ulva* (term/family present in the *Ulva* bacterial genome but not present in the seawater bacterial genome) divided by the number of discordant pairs in favor of seawater (term/family present in the seawater bacterial genome but not present in the *Ulva* bacterial genome). An offset of 0.5 was added to the number of discordant pairs to prevent dividing by zero. As multiple genomes were available per genus, pairs were randomly assigned 1000 times (permutations) and odds ratios were calculated for each permutation. The median odds ratio was retained. A term/family more frequent in *Ulva* bacterial genomes results in an odds ratio larger than one. The opposite results in an odds ratio smaller than one.

All statistical tests were performed in R (*95*), and data were visualized using the ggplot2 (*96*) and phyloseq (*97*) packages.

Supplementary Materials

The PDF file includes:
Legends for tables S1 to S4

Other Supplementary Material for this manuscript includes the following:
Tables S1 to S4

REFERENCES AND NOTES

1. S. Egan, T. Harder, C. Burke, P. Steinberg, S. Kjelleberg, T. Thomas, The seaweed holobiont: Understanding seaweed-bacteria interactions. *FEMS Microbiol. Rev.* **37**, 462–476 (2013).
2. L. M. van der Loos, B. K. Eriksson, J. Falcão Salles, The macroalgal holobiont in a changing sea. *Trends Microbiol.* **27**, 635–650 (2019).
3. J. Li, M. E. Majzoub, E. M. Marzinelli, Z. Dai, T. Thomas, S. Egan, Bacterial controlled mitigation of dysbiosis in a seaweed disease. *ISME J.* **16**, 378–387 (2022).
4. M. Gemin, A. Peña-Rodríguez, E. Quiroz-Guzmán, P. Magallón-Servín, D. Barajas-Sandoval, R. Elizondo-González, Growth-promoting bacteria for the green seaweed *Ulva clathrata*. *Aquac. Res.* **50**, 3741–3748 (2019).
5. C. Riquelme, A. Rojas, V. Flores, J. A. Correa, Epiphytic bacteria in a copper-enriched environment in northern Chile. *Mar. Pollut. Bull.* **34**, 816–820 (1997).
6. T. Wichard, B. Charrier, F. Mineur, J. H. Bothwell, O. De Clerck, J. C. Coates, The green seaweed *Ulva*: A model system to study morphogenesis. *Front. Plant Sci.* **6**, 72 (2015).
7. L. Provasoli, Effect of plant hormones on *Ulva*. *Biol. Bull.* **114**, 375–384 (1958).
8. M. Spoerner, T. Wichard, T. Bachhuber, J. Stratmann, W. Oertel, Growth and thallus morphogenesis of *Ulva mutabilis* (Chlorophyta) depends on a combination of two bacterial species excreting regulatory factors. *J. Phycol.* **48**, 1433–1447 (2012).
9. J. Grueneberg, A. H. Engelen, R. Costa, T. Wichard, Macroalgal morphogenesis induced by waterborne compounds and bacteria in coastal seawater. *PLOS ONE* **11**, e0146307 (2016).
10. L. M. van der Loos, C. De Wilde, A. Willems, O. De Clerck, S. Steinhagen, The cultivated sea lettuce (*Ulva*) microbiome: Successional and seasonal dynamics. *Aquaculture* **585**, 740692 (2024).
11. K. M. Davis, L. Zeinert, A. Byrne, J. Davis, C. Roemer, M. Wright, L. W. Parfrey, Successional dynamics of the cultivated kelp microbiome. *J. Phycol.* **59**, 538–551 (2023).
12. L. Düsedau, Y. Ren, M. Hou, M. Wahl, Z.-M. Hu, G. Wang, F. Weinberger, Elevated temperature-induced epimicrobiome shifts in an invasive seaweed *Gracilaria vermiculophylla*. *Microorganisms* **11**, 599 (2023).
13. B. Paix, P. Potin, G. Schires, C. Le Poupon, B. Misson, C. Leblanc, G. Culioli, J.-F. Briand, Synergistic effects of temperature and light affect the relationship between *Taonia atomaria* and its epibacterial community: A controlled conditions study. *Environ. Microbiol.* **23**, 6777–6797 (2021).
14. C. Dai, S. Wang, The structure and function of the *Sargassum fusiforme* microbiome under different conditions. *J. Mar. Sci. Eng.* **10**, 1401 (2022).
15. B. Glasl, J. B. Haskell, T. Aires, E. A. Serrão, D. G. Bourne, N. S. Webster, P. R. Frade, Microbial surface biofilm responds to the growth-reproduction-senescence cycle of the dominant coral reef macroalgae *Sargassum* spp. *Life* **11**, 1199 (2021).
16. J. Wang, X. Tang, Z. Mo, Y. Mao, Metagenome-assembled genomes from *Pyropia haitanensis* microbiome provide insights into the potential metabolic functions to the seaweed. *Front. Microbiol.* **13**, 857901 (2022).
17. B. L. Weigel, K. K. Miranda, E. C. Fogarty, A. R. Watson, C. A. Pfister, Functional insights into the kelp microbiome from metagenome-assembled genomes. *mSystems* **7**, e0142221 (2022).
18. K. M. Rath, N. Fierer, D. V. Murphy, J. Rousk, Linking bacterial community composition to soil salinity along environmental gradients. *ISME J.* **13**, 836–846 (2019).
19. S. Steinhagen, S. Hoffmann, H. Pavia, G. B. Toth, Molecular identification of the ubiquitous green algae *Ulva* reveals high biodiversity, crypticity, and invasive species in the Atlantic-Baltic Sea region. *Algal Res.* **73**, 103132 (2023).
20. L. M. van der Loos, S. D'hondt, A. H. Engelen, H. Pavia, G. B. Toth, A. Willems, F. Weinberger, O. De Clerck, S. Steinhagen, Salinity and host drive *Ulva*-associated bacterial communities across the Atlantic-Baltic Sea gradient. *Mol. Ecol.* **32**, 6260–6277 (2023).
21. C. A. Lozupone, R. Knight, Global patterns in bacterial diversity. *Proc. Natl. Acad. Sci. U.S.A.* **104**, 11436–11440 (2007).
22. B. L. Cantarel, P. M. Coutinho, C. Rancurel, T. Bernard, V. Lombard, B. Henrissat, The Carbohydrate-Active EnZymes database (CAZy): An expert resource for glycogenomics. *Nucleic Acids Res.* **37**, D233–D238 (2009).
23. M. Kanehisa, S. Goto, KEGG: Kyoto Encyclopedia of Genes and Genomes. *Nucleic Acids Res.* **28**, 27–30 (2000).
24. M. Kanehisa, M. Araki, S. Goto, M. Hattori, M. Hirakawa, M. Itoh, T. Katayama, S. Kawashima, S. Okuda, T. Tokimatsu, Y. Yamanishi, KEGG for linking genomes to life and the environment. *Nucleic Acids Res.* **36**, D480–D484 (2008).
25. N. Wahlström, F. Nylander, E. Malmhäll-Bah, K. Sjövold, U. Edlund, G. Westman, E. Albers, Composition and structure of cell wall ulvans recovered from *Ulva* spp. along the Swedish west coast. *Carbohydr. Polym.* **233**, 115852 (2020).
26. Y. Yang, M. Zhang, A. I. Alalawy, F. M. Almutairi, M. A. Al-Duais, J. Wang, E.-S. Salama, Identification and characterization of marine seaweeds for biocompounds production. *Environ. Technol. Innov.* **24**, 101848 (2021).
27. S. Scholz, M. Serif, D. Schleheck, M. D. J. Sayer, A. M. Cook, F. C. Küpper, Sulfoquinovose metabolism in marine algae. *Bot. Mar.* **64**, 301–312 (2021).
28. L. Han, G.-P. Yang, C.-Y. Liu, Y.-M. Jin, T. Liu, Emissions of biogenic sulfur compounds and their regulation by nutrients during an *Ulva prolifera* bloom in the Yellow Sea. *Mar. Pollut. Bull.* **162**, 111885 (2021).
29. K. L. Van Alstyne, L. Koellermeier, T. A. Nelson, Spatial variation in dimethylsulfoniopropionate (DMSP) production in *Ulva lactuca* (Chlorophyta) from the Northeast Pacific. *Mar. Biol.* **150**, 1127–1135 (2007).
30. R. W. Kessler, A. Weiss, S. Kuegler, C. Hermes, T. Wichard, Macroalgal–bacterial interactions: Role of dimethylsulfoniopropionate in microbial gardening by *Ulva* (Chlorophyta). *Mol. Ecol.* **27**, 1808–1819 (2018).

31. J. T. Kidgell, M. Magnusson, R. de Nys, C. R. K. Glasson, Ulvan: A systematic review of extraction, composition and function. *Algal Res.* **39**, 101422 (2019).
32. T. Tang, S. Cao, B. Zhu, Q. Li, Ulvan polysaccharide-degrading enzymes: An updated and comprehensive review of sources category, property, structure, and applications of ulvan lyases. *Algal Res.* **60**, 102477 (2021).
33. L. Reisky, C. Stanetty, M. D. Mihovilovic, T. Schweder, J. H. Hehemann, U. T. Bornscheuer, Biochemical characterization of an ulvan lyase from the marine flavobacterium *Formosa agariphila* KMM 3901T. *Appl. Microbiol. Biotechnol.* **102**, 6987–6996 (2018).
34. S. Steinhagen, K. Stedt, J. P. Trigo, I. Undeland, H. Pavia, A step towards closing the food-waste gap in novel protein sources: Post-harvest protein boost of the seaweed crop *Ulva* by herring production tub water. *Future Foods* **9**, 100347 (2024).
35. A. C. Tyler, K. J. McGlathery, I. C. Anderson, Benthic algae control sediment—Water column fluxes of organic and inorganic nitrogen compounds in a temperate lagoon. *Limnol. Oceanogr.* **48**, 2125–2137 (2003).
36. H. Li, Y. Zhang, J. Chen, X. Zheng, F. Liu, N. Jiao, Nitrogen uptake and assimilation preferences of the main green tide alga *Ulva prolifera* in the Yellow Sea, China. *J. Appl. Phycol.* **31**, 625–635 (2019).
37. A. C. Tyler, K. J. McGlathery, S. A. Macko, Uptake of urea and amino acids by the macroalgae *Ulva lactuca* (Chlorophyta) and *Gracilaria vermiculophylla* (Rhodophyta). *Mar. Ecol. Prog. Ser.* **294**, 161–172 (2005).
38. L. S. de Oliveira, G. B. Gregoracci, G. G. Z. Silva, L. T. Salgado, G. A. Filho, M. Alves-ferreira, R. C. Pereira, F. L. Thompson, Transcriptomic analysis of the red seaweed *Laurencia dendroidea* (Florideophyceae, Rhodophyta) and its microbiome. *BMC Genomics* **13**, 487 (2012).
39. Y. Xiong, R. Yang, X. Sun, H. Yang, H. Chen, Effect of the epiphytic bacterium *Bacillus* sp. WPySW2 on the metabolism of *Pyropia haitanensis*. *J. Appl. Phycol.* **30**, 1225–1237 (2018).
40. K. J. Flynn, C. R. N. Wright, The simultaneous assimilation of ammonium and l-arginine by the marine diatom *Phaeodactylum tricornutum* Bohlin. *J. Exp. Mar. Biol. Ecol.* **95**, 257–269 (1986).
41. F. Linares, Effect of dissolved free amino acids (DFAA) on the biomass and production of microphytobenthic communities. *J. Exp. Mar. Biol. Ecol.* **330**, 469–481 (2006).
42. J. G. LeBlanc, C. Milani, G. S. De Giori, F. Sesma, D. Van Sinderen, M. Ventura, Bacteria as vitamin suppliers to their host: A gut microbiota perspective. *Curr. Opin. Biotechnol.* **24**, 160–168 (2013).
43. B. Ryback, M. Bortfeld-Miller, J. A. Vorholt, Metabolic adaptation to vitamin auxotrophy by leaf-associated bacteria. *ISME J.* **16**, 2712–2724 (2022).
44. M. T. Croft, A. D. Lawrence, E. Raux-Deery, M. J. Warren, A. G. Smith, Algae acquire vitamin B_{12} through a symbiotic relationship with bacteria. *Nature* **438**, 90–93 (2005).
45. M. R. Droop, Vitamin B_{12} in marine ecology. *Nature* **180**, 1041–1042 (1957).
46. L. Fries, Requirements for organic substances in seaweeds. *Bot. Mar.* **16**, 19–31 (1973).
47. M. T. Croft, M. J. Warren, A. G. Smith, Algae need their vitamins. *Eukaryot. Cell* **5**, 1175–1183 (2006).
48. A. F. Mohsen, A. F. Khaleafa, M. A. Hashem, A. Metwalli, Effect of some vitamins on growth, reproduction, amino acid, fat and sugar contents in *Ulva fasciata* Delile (Part I). *Bot. Mar.* **17**, 208–212 (1974).
49. A. H. Nasr, I. A. Bekheet, The effect of some organic micronutrients on some marine algae from Alexandria. *Hydrobiologia* **34**, 295–304 (1969).
50. L. S. Jahnke, A. L. White, Long-term hyposaline and hypersaline stresses produce distinct antioxidant responses in the marine alga *Dunaliella tertiolecta*. *J. Plant Physiol.* **160**, 1193–1202 (2003).
51. P. García-Caparrós, M. Hasanuzzaman, M. T. Lao, "Oxidative stress and antioxidant defense in plants under salinity" in *Reactive Oxygen, Nitrogen and Sulfur Species in Plants*, M. Hasanuzzaman, V. Fotopoulos, K. Nahar, M. Fujita, Eds. (Wiley, ed. 1, 2019), pp. 291–309.
52. M. Gurumurthy, M. Rao, T. Mukherjee, S. P. S. Rao, H. I. Boshoff, T. Dick, C. E. Barry III, U. H. Manjunatha, A novel F_{420}-dependent anti-oxidant mechanism protects *Mycobacterium tuberculosis* against oxidative stress and bactericidal agents. *Mol. Microbiol.* **87**, 744–755 (2013).
53. R. Grinter, C. Greening, Cofactor F_{420}: An expanded view of its distribution, biosynthesis and roles in bacteria and archaea. *FEMS Microbiol. Rev.* **45**, fuab021 (2021).
54. M. Rapala-Kozik, N. Wolak, M. Kujda, A. K. Banas, The upregulation of thiamine (vitamin B_1) biosynthesis in *Arabidopsis thaliana* seedlings under salt and osmotic stress conditions is mediated by abscisic acid at the early stages of this stress response. *BMC Plant Biol.* **12**, 2 (2012).
55. A. A. Mosavikia, S. G. Mosavi, M. Seghatoleslami, R. Baradaran, Chitosan nanoparticle and pyridoxine seed priming improves tolerance to salinity in milk thistle seedling. *Not. Bot. Horti Agrobot. Cluj Napoca* **48**, 221–233 (2020).
56. A. A. Faarghl, Thiamine and pyridoxine alleviate oxidative damage by copper stress in green alga *Chlorella vulgaris*. *Egypt. J. Microbiol.* **47**, 97–110 (2012).
57. L. L. Fern, A. A. Z. Abidin, Z. N. B. Yusof, Upregulation of thiamine (vitamin B_1) biosynthesis gene upon stress application in *Anabaena* sp. and *Nannochloropsis oculata*. *J. Plant Biotechnol.* **44**, 462–471 (2017).
58. R. Liu, Q. N. Zhang, J. Lu, C. H. Zhang, L. Zhang, Y. Wu, The effects of exogenous pyridoxal-5-phosphate on seedling growth and development of wheat under salt stress. *Cereal Res. Commun.* **47**, 442–454 (2019).
59. S. Hussain, J. Huang, C. Zhu, L. Zhu, X. Cao, S. Hussain, M. Ashraf, M. A. Khaskheli, Y. Kong, Q. Jin, X. Li, J. Zhang, Pyridoxal 5′-phosphate enhances the growth and morpho-physiological characteristics of rice cultivars by mitigating the ethylene accumulation under salinity stress. *Plant Physiol. Biochem.* **154**, 782–795 (2020).
60. E. L. McParland, H. Alexander, W. M. Johnson, The osmolyte ties that bind: Genomic insights into synthesis and breakdown of organic osmolytes in marine microbes. *Front. Mar. Sci.* **8**, 689306 (2021).
61. R. D. Sleator, C. Hill, Bacterial osmoadaptation: The role of osmolytes in bacterial stress and virulence. *FEMS Microbiol. Rev.* **26**, 49–71 (2002).
62. X. Hu, D. Li, Y. Qiao, Q. Song, Z. Guan, K. Qiu, J. Cao, L. Huang, Salt tolerance mechanism of a hydrocarbon-degrading strain: Salt tolerance mediated by accumulated betaine in cells. *J. Hazard. Mater.* **392**, 122326 (2020).
63. C. L. Dupont, J. Larsson, S. Yooseph, K. Ininbergs, J. Goll, J. Asplund-Samuelsson, J. P. McCrow, N. Celepli, L. Z. Allen, M. Ekman, A. J. Lucas, Å. Hagström, M. Thiagarajan, B. Brindefalk, A. R. Richter, A. F. Andersson, A. Tenney, D. Lundin, A. Tovchigrechko, J. A. A. Nylander, D. Brami, J. H. Badger, A. E. Allen, D. B. Rusch, J. Hoffman, E. Norrby, R. Friedman, J. Pinhassi, J. C. Venter, B. Bergman, Functional tradeoffs underpin salinity-driven divergence in microbial community composition. *PLOS ONE* **9**, e89549 (2014).
64. G. O. Kirst, Salinity tolerance of eukaryotic marine algae. *Annu. Rev. Plant. Physiol. Plant. Mol. Biol.* **40**, 21–53 (1989).
65. Q. Xing, G. Bi, M. Cao, A. Belcour, M. Aite, Z. Mo, Y. Mao, Comparative transcriptome analysis provides insights into response of *Ulva compressa* to fluctuating salinity conditions. *J. Phycol.* **57**, 1295–1308 (2021).
66. Z. N. A. Hattab, S. A. Al-Ajeel, E. A. J. El-Kaaby, Effect of salinity stress on *Capsicum annuum* callus growth, regeneration and callus content of capsaicin, phenylalanine, proline and ascorbic acid. *J. Life Sci.* **10**, 304–310 (2015).
67. S. M. Dittami, A. Gravot, D. Renault, S. Goulitquer, A. Eggert, A. Bouchereau, C. Boyen, T. Tonon, Integrative analysis of metabolite and transcript abundance during the short-term response to saline and oxidative stress in the brown alga *Ectocarpus siliculosus*. *Plant Cell Environ.* **34**, 629–642 (2011).
68. N. Zahra, Z. A. Raza, S. Mahmood, Effect of salinity stress on various growth and physiological attributes of two contrasting maize genotypes. *Braz. Arch. Biol. Technol.* **63**, e20200072 (2020).
69. R. Oshone, M. Ngom, F. Chu, S. Mansour, M. O. Sy, A. Champion, L. S. Tisa, Genomic, transcriptomic, and proteomic approaches towards understanding the molecular mechanisms of salt tolerance in *Frankia* strains isolated from Casuarina trees. *BMC Genomics* **18**, 633 (2017).
70. D. A. Los, N. Murata, Membrane fluidity and its roles in the perception of environmental signals. *Biochim. Biophys. Acta BBA Biomembr.* **1666**, 142–157 (2004).
71. D. C. Sévin, J. N. Stählin, G. R. Pollak, A. Kuehne, U. Sauer, Global metabolic responses to salt stress in fifteen species. *PLOS ONE* **11**, e0148888 (2016).
72. D. C. Sévin, U. Sauer, Ubiquinone accumulation improves osmotic-stress tolerance in *Escherichia coli*. *Nat. Chem. Biol.* **10**, 266–272 (2014).
73. V. Agmo Hernández, E. K. Eriksson, K. Edwards, Ubiquinone-10 alters mechanical properties and increases stability of phospholipid membranes. *Biochim. Biophys. Acta BBA Biomembr.* **1848**, 2233–2243 (2015).
74. J. Šajbidor, Effect of some environmental factors on the content and composition of microbial membrane lipids. *Crit. Rev. Biotechnol.* **17**, 87–103 (1997).
75. H. Goldfine, Bacterial membranes and lipid packing theory. *J. Lipid Res.* **25**, 1501–1507 (1984).
76. O. Geiger, I. M. López-Lara, C. Sohlenkamp, Phosphatidylcholine biosynthesis and function in bacteria. *Biochim. Biophys. Acta BBA Mol. Cell Biol. Lipids* **1831**, 503–513 (2013).
77. A. S. Alves, H. Adão, J. Patrício, J. M. Neto, M. J. Costa, J. C. Marques, Spatial distribution of subtidal meiobenthos along estuarine gradients in two southern European estuaries (Portugal). *J. Mar. Biol. Assoc. U. K.* **89**, 1529–1540 (2009).
78. S. Kieser, J. Brown, E. M. Zdobnov, M. Trajkovski, L. A. McCue, ATLAS: A Snakemake workflow for assembly, annotation, and genomic binning of metagenome sequence data. *BMC Bioinformatics* **21**, 257 (2020).
79. B. Bushnell, BBTools (2019); https://sourceforge.net/projects/bbmap/.
80. O. De Clerck, S. M. Kao, K. A. Bogaert, J. Blomme, F. Foflonker, M. Kwantes, E. Vancaester, L. Vanderstraeten, E. Aydogdu, J. Boesger, G. Califano, B. Charrier, R. Clewes, A. Del Cortona, S. D'Hondt, N. Fernandez-Pozo, C. M. Gachon, M. Hanikenne, L. Lattermann, F. Leliaert, X. Liu, C. A. Maggs, Z. A. Popper, J. A. Raven, M. Van Bel, P. K. I. Wilhelmsson, D. Bhattacharya, J. C. Coates, S. A. Rensing, D. Van Der Straeten, A. Vardi, L. Sterck, K. Vandepoele, Y. Van de Peer, T. Wichard, J. H. Bothwell, Insights into the evolution of multicellularity from the sea lettuce genome. *Curr. Biol.* **28**, 2921–2933.e5 (2018).
81. D. Li, R. Luo, C.-M. Liu, C.-M. Leung, H.-F. Ting, K. Sadakane, H. Yamashita, T.-W. Lam, MEGAHIT v1.0: A fast and scalable metagenome assembler driven by advanced methodologies and community practices. *Methods* **102**, 3–11 (2016).
82. D. D. Kang, F. Li, E. Kirton, A. Thomas, R. Egan, H. An, Z. Wang, MetaBAT 2: An adaptive binning algorithm for robust and efficient genome reconstruction from metagenome assemblies. *PeerJ* **7**, e7359 (2019).

83. Y.-W. Wu, B. A. Simmons, S. W. Singer, MaxBin 2.0: An automated binning algorithm to recover genomes from multiple metagenomic datasets. *Bioinformatics* **32**, 605–607 (2016).
84. C. M. K. Sieber, A. J. Probst, A. Sharrar, B. C. Thomas, M. Hess, S. G. Tringe, J. F. Banfield, Recovery of genomes from metagenomes via a dereplication, aggregation and scoring strategy. *Nat. Microbiol.* **3**, 836–843 (2018).
85. D. H. Parks, M. Imelfort, C. T. Skennerton, P. Hugenholtz, G. W. Tyson, CheckM: Assessing the quality of microbial genomes recovered from isolates, single cells, and metagenomes. *Genome Res.* **25**, 1043–1055 (2015).
86. M. R. Olm, C. T. Brown, B. Brooks, J. F. Banfield, dRep: A tool for fast and accurate genomic comparisons that enables improved genome recovery from metagenomes through de-replication. *ISME J.* **11**, 2864–2868 (2017).
87. D. H. Parks, M. Chuvochina, D. W. Waite, C. Rinke, A. Skarshewski, P.-A. Chaumeil, P. Hugenholtz, A standardized bacterial taxonomy based on genome phylogeny substantially revises the tree of life. *Nat. Biotechnol.* **36**, 996–1004 (2018).
88. D. Hyatt, G.-L. Chen, P. F. LoCascio, M. L. Land, F. W. Larimer, L. J. Hauser, Prodigal: Prokaryotic gene recognition and translation initiation site identification. *BMC Bioinformatics* **11**, 119 (2010).
89. M. Steinegger, J. Söding, Clustering huge protein sequence sets in linear time. *Nat. Commun.* **9**, 2542 (2018).
90. J. Huerta-Cepas, K. Forslund, L. P. Coelho, D. Szklarczyk, L. J. Jensen, C. Von Mering, P. Bork, Fast genome-wide functional annotation through orthology assignment by eggNOG-mapper. *Mol. Biol. Evol.* **34**, 2115–2122 (2017).
91. J. Oksanen, F. G. Blanchet, M. Friendly, R. Kindt, P. Legendre, D. McGlinn, P. R. Minchin, R. B. O'Hara, G. L. Simpson, P. Solymos, M. H. H. Stevens, E. Szoecs, H. Wagner, Vegan: Community ecology package. R package version 2.5-7 (CRAN, 2020).
92. P. Martinez Arbizu, pairwiseAdonis: Pairwise multilevel comparison using adonis, R package version 0.4, Github (2020); https://github.com/pmartinezarbizu/pairwiseAdonis.
93. H. Zhou, K. He, J. Chen, X. Zhang, LinDA: Linear models for differential abundance analysis of microbiome compositional data. *Genome Biol.* **23**, 95 (2022).
94. G. B. Gloor, J. M. Macklaim, V. Pawlowsky-Glahn, J. J. Egozcue, Microbiome datasets are compositional: And this is not optional. *Front. Microbiol.* **8**, 2224 (2017).
95. R Core Team, R: A language and environment for statistical computing (R Foundation for Statistical Computing, 2020); https://r-project.org/.
96. H. Wickham, Ggplot2: Elegant Graphics for Data Analysis (Springer-Verlag, 2016); https://ggplot2.tidyverse.org).
97. P. J. McMurdie, S. Holmes, Phyloseq: An R package for reproducible interactive analysis and graphics of microbiome census data. *PLOS ONE* **8**, e61217 (2013).

Acknowledgments: We would like to thank S. Hoffmann for assistance during field work and N. Stärck for assistance with nutrient analyses. **Funding:** The research leading to the results presented in this publication was carried out with infrastructure funded by the FWO PhD Fellowship fundamental research (3F020119), the EMBRC Belgium (FWO project I001621N), and the Formas-funded "A manual for the use of sustainable marine resources" project (grant no. 2022-00331). W.S. is funded through the FWO grant no. 1252821N. **Author contributions:** Conceptualization: S.D., O.D.C., S.S., and L.M.v.d.L. Methodology: S.D., O.D.C., and L.M.v.d.L. Investigation: S.D., O.D.C., and S.S. Formal analysis: W.S. and L.M.v.d.L. Software: W.S. Data curation: L.M.v.d.L. Writing—original draft: L.M.v.d.L. Writing—review and editing: S.D., F.W., O.D.C., S.S., W.S., and A.W. Visualization: O.D.C. and L.M.v.d.L. Validation: S.D. and S.S.. Funding acquisition: O.D.C., S.S., and A.W. Resources: S.D., F.W., O.D.C., S.S., and W.S. Supervision: O.D.C. and A.W. Project administration: O.D.C. **Competing interests:** The authors declare that they have no competing interests. **Data and materials availability:** All data needed to evaluate the conclusions in the paper are present in the paper and/or the Supplementary Materials. Raw metagenomic sequence reads and related metadata are deposited in the SRA (BioProject PRJNA1040445).

Submitted 9 July 2024
Accepted 17 December 2024
Published 17 January 2025
10.1126/sciadv.adr6070